Impact of wetting-layer density of states on the carrier relaxation process in low indium content self-assembled (In,Ga)As/GaAs quantum dots

M. Syperek,* M. Baranowski, G. Sęk, and J. Misiewicz
Institute of Physics, Wrocław Uniwersity of Technology, Wybrzeże Wyspiańskiego 27, 50-370 Wrocław, Poland

A. Löffler, S. Höfling, S. Reitzenstein,† M. Kamp, and A. Forchel
Technische Physik, Universität Würzburg and Wilhelm Conrad Röntgen Research Center for Complex Material Systems, Am Hubland, D-97074 Würzburg, Germany

(Received 22 May 2012; revised manuscript received 31 December 2012; published 11 March 2013)

Carrier relaxation processes have been studied in low indium content self-assembled (In,Ga)As/GaAs quantum dots (QDs). Temperature-dependent photoluminescence of the wetting layer (WL) and QDs, and QD photoluminescence rise time elongation from ∼100 to ∼200 ps in the range of 10–45 K, indicated a complex carrier relaxation scheme. It involves localization of carriers/excitons in the WL, their temperature-mediated release, and subsequent transfer between the states of the WL and QD ensemble. These observations are explained by a thermal hopping model, in which electron-hole pairs are redistributed within two separate sets of zero-dimensional states of considerably different densities connected by a two-dimensional mobility channel.

DOI: 10.1103/PhysRevB.87.125305 PACS number(s): 78.67.Hc, 78.47.D−, 78.55.Cr

I. INTRODUCTION

The rapid development in the fabrication of self-assembled semiconductor quantum dot (QD) structures has been followed by a remarkable amount of research devoted to the exploration of their unique electronic and optical properties.[1,2] The quasi-zero-dimensional character of the QD density of states and possibilities to achieve dense QD matrices as well as single QD objects open a broad field of potential applications.[3,4] As long as low-temperature operation is taken into account, which is justified for some of the very sophisticated quantum devices, the considered QD system containing lowly strained and elongated (enlarged) quantum dots exemplifies one of the possible target systems for optoelectronic devices utilizing cavity quantum electrodynamics. Its peculiar properties, such as low QD surface density and enhanced transition oscillator strength, can lead to the development of a dot-in-cavity system characterized by a superior photon extraction efficiency, highly directed emission, a tunable photon emission rate, and easily reachable strong-coupling regime conditions for moderate quality factors of the cavities. These are related to at least a few applications, starting from single-dot lasers, single-dot photon emitters, quantum information processing devices based on single QDs, QD molecules, and QD matrices.[5–9] For most of these foreseen applications, the knowledge of carrier dynamics, including carrier diffusion, QD carrier capture, and intraband relaxation to the QD ground state, plays a pivotal role.

Self-assembled QDs grown in the Stranski-Krastanow mode are formed on a strained wetting layer (WL), being nominally a few-monolayers-thick quantum well. For nonequilibrium carrier population injected into the matrix (GaAs in this case), its relaxation down to the QD ground state can occur either (i) directly,[10] (ii) through the continuum of the band gap states,[11–14] or (iii) through the WL.[15–22] It is well established that the carrier-phonon[23–25] and Coulomb inelastic scattering[25–28] processes among others provide efficient channels of energy dissipation in all these cases. The relaxation of photogenerated carriers into QDs via the wetting layer has been widely investigated so far, revealing its key role in the relaxation scheme.[15–22] This research affirms that the WL can act as a large carrier reservoir, collecting electrons and holes from the matrix and redistributing them over the ensemble of QDs. The relaxation scenario, however, strongly depends on the nature of the WL carrier confinement, especially when taking into account the 0D WL carrier localization,[18,29–33] and it still remains unclear in many systems.

In this paper, we study the temperature-affected carrier relaxation dynamics and its dependence on the surface density of dots and density of states in the wetting layer, in a sample containing low strain $In_{0.3}Ga_{0.7}As$ QDs. The relaxation processes are probed directly by photoluminescence (PL) and picosecond time-resolved photoluminescence (TRPL) measurements performed as a function of temperature.

We identify a significant role of the carrier localization in the WL due to its local confinement potential fluctuations, and its influence on the carrier relaxation in the entire system. Moreover, we show that the ratio between the density of such quasi-zero-dimensional states in the WL and the surface density of QDs has a major influence on the carrier dynamics and can lead to an atypical elongation of the QD PL rise time with temperature.

II. EXPERIMENT

The sample was grown by solid source molecular beam epitaxy on an undoped (001) oriented GaAs substrate. A weakly strained $In_{0.3}Ga_{0.7}As$ layer with a nominal thickness of 4.5 nm was deposited on a 300-nm-thick GaAs buffer. Due to the strain release and surface atom migration anisotropy, strongly elongated QDs are formed, with typical sizes of 25 nm in width, several nanometers in height, and up to 100 nm in length for uncapped QDs.[34,35] They are preferentially aligned along the $[1\bar{1}0]$ direction and exhibit a rather low planar density of $\sim 5\times 10^9$ cm^{-2}. For the PL and TRPL experiments, the sample was placed in a helium-flow cryostat with a precise (better than 0.1 K) control of the temperature in the range of

4.5–300 K. The structure was excited nonresonantly by a pulse train from a Ti:sapphire mode-locked laser with a repetition frequency of 76 MHz and 140 fs pulse width. The intensity of the emitted light was detected by a liquid-nitrogen-cooled (In,Ga)As charge-coupled device camera combined with a 0.3 m focal length single grating monochromator. In the case of TRPL experiment, the temporal characteristics of the PL intensity was analyzed by a streak camera system equipped with the S1 photocathode. The effective time resolution of the setup was ∼15 ps.

III. EXPERIMENTAL RESULTS

A. Photoluminescence

Figure 1(a) shows the evolution of the PL spectra versus temperature for the $In_{0.3}Ga_{0.7}As/GaAs$ QDs under nonresonant excitation with photon energy of 1.557 eV. At $T = 10$ K, the PL spectrum is dominated by a peak centered at 1.347 eV, which exhibits some asymmetry toward the low-energy side. With increasing temperature, the asymmetry increases and finally at $T > 30$ K two well-resolved PL bands appear. This finding suggests that in the considered temperature range of 10–60 K, the PL spectrum always consists of at least two main emission channels. The high-energy one is attributed to the electron-hole recombination in the WL, whereas the lower-energy emission is related to the QD ensemble. For further analysis, the PL spectrum was fitted by two Gaussian profiles. For each of them, the integrated emission intensity and the energy position of the PL maximum was extracted; both are illustrated in Fig. 1. As can be seen in Fig. 1(b), when the temperature increases from 10 K to ∼30 K, the emission intensity of the WL band quenches considerably while the QD emission intensity increases. Such correlation between the WL and QD PL intensities indicates the existence of a temperature-activated carrier transfer process between two different sets of optically active states (in the WL and QDs).

Another striking feature is observed in Fig. 1(c). The WL PL peak position is almost constant at 1.347 eV in the temperature range from 10 to 30 K and it shifts slightly to higher energy for $T > 30$ K, whereas for the QD emission there is observed a continuous shift of the PL peak maximum toward lower

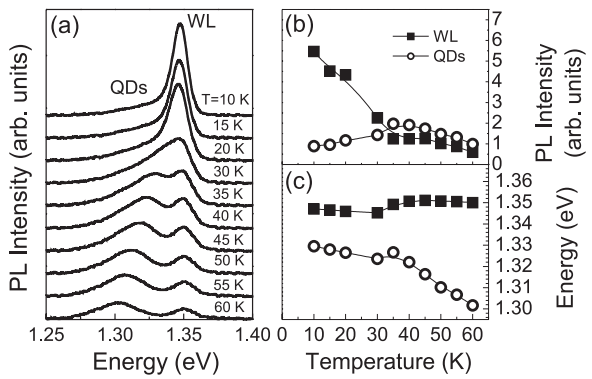

FIG. 1. (a) PL spectra evolution vs temperature obtained for $In_{0.3}Ga_{0.7}As/GaAs$ QD structure. (b) Temperature dependence of the integrated PL intensity for the WL (full squares) and QD (open circles). (c) Energy position of the peak maximum vs temperature for the WL and QDs PL bands.

energy as the temperature increases. The latter is caused by the temperature-driven spatial redistribution of carriers between QDs of different quantum confinement depths. Note that the excitation conditions used here ($P_{av} = 0.5$ W cm^{-2}) correspond to less than 1 electron-hole (e-h) pair created per dot within a pulse, i.e., not all the dots are populated on average. Contrary to QDs, a slight spectral blueshift of the WL emission energy can be related to the carrier release from the localized WL states to the 2D WL mobility edge (extended 2D states).

The above-presented analysis allows us to draw a consistent picture of the carrier dynamics in the investigated QD sample. Just after the optical pulse excitation, the photogenerated electron-hole pairs relax from the GaAs matrix down to the WL and QDs. Since the WL PL intensity dominates the overall PL spectrum at low T, the majority carrier population is efficiently collected by the WL, which has in addition a complex density of states (DOS). Our previous μPL experiments confirmed that a three-dimensional carrier confinement is present in the WL, dominating the PL spectrum at low temperatures.[36] Indeed, the expected two-dimensional WL density of states (2D DOS) is accompanied by a zero-dimensional one (0D DOS). The 0D WL states have previously been observed in self-assembled InAs/GaAs (Ref. 33) and (In,Al)As/(Al,Ga)As (Ref. 31) QD structures. Their presence can be attributed to the clustering effect occurring especially at the border between the 2D and 3D surface morphology transition in Stranski-Krastanow growth mode.[29] Another explanation of 0D WL state formation is the local variation in the WL chemical composition (In variation[33]) and WL thickness. We believe that both these effects are most likely present in our QD structure.

Let us turn back to the carrier relaxation scenario. Since we kept low the density of the photogenerated e-h pair population, the increase in the temperature enhances the phonon-mediated rather than the inelastic Coulomb scattering carrier transport, which in turn contributes to (i) carrier redistribution between 0D WL states, (ii) carrier activation from 0D states to the 2D WL mobility edge, and (iii) carrier capture and redistribution within the ensemble of dots.

B. Time-resolved photoluminescence

The carrier relaxation scenario described above can be verified more directly by measuring the PL signal kinetics. Figure 2 shows examples of the TRPL traces measured in the spectral region corresponding to the WL emission [Fig. 2(a)] and the QD emission [Fig. 2(c)]. Each TRPL trace was fitted with a double exponential function in order to extract the PL rise, τ_R^i, and decay time constants, τ_D^i, respectively, for the WL ($i = \mathrm{WL}$) and QDs ($i = \mathrm{QD}$). The τ_D^{WL} and τ_D^{QD} versus temperature are presented in Fig. 2(d). At $T = 10$ K, $\tau_D^{WL} \approx 280$ ps and drops slightly within the entire investigated temperature range, while τ_D^{QD} increases from 350 at 10 K to reach the maximum of ∼500 ps at 35–45 K, and finally drops down to ∼380 ps at 60 K. The low-temperature QD PL decay agrees well with the exciton recombination time of 350 ps measured for a similar, elongated $In_{0.3}Ga_{0.7}As$ QDs by a single photon counting method.[37] The most intriguing result is observed for the PL rise time as presented in Fig. 2(b). While the τ_R^{WL} shows a reduction from 50 ps down to 15 ps when the temperature increases, the QD PL rise time exhibits

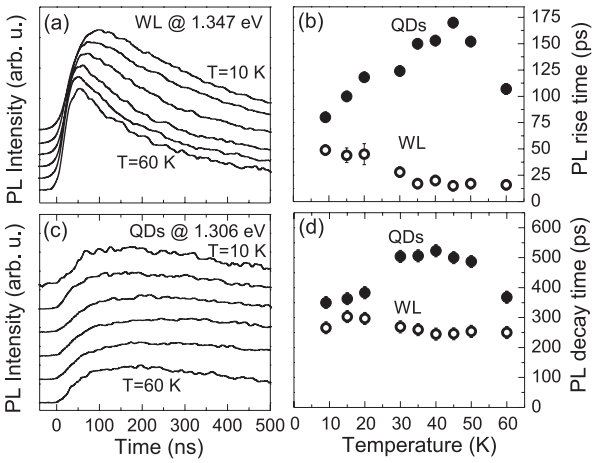

FIG. 2. (a) TRPL traces vs temperature for the WL emission at 1.347 eV, and (c) QD emission at 1.306 eV. (b) Temperature dependence of the WL and QDs PL rise time, and (d) PL decay time. Excitation power $P_{av} = 0.5$ W cm^{-2}.

a considerable increase from 70 ps at 10 K up to ∼160 ps at 45 K. The τ_R^{QD} characterizes the *e-h* population built-up time at the QD ground state.[38] Such a rise time elongation has been observed experimentally in other structures,[39–43] but it has never been explained satisfactorily before.

IV. THEORETICAL MODEL OF CARRIER KINETICS

A. Model introduction and general assumptions

To explain the experimentally observed carrier kinetics, we propose a simple multilevel model based on the above-mentioned relaxation scheme illustrated in Fig. 3. In this sense, it resembles to some extent the Mott conductivity model introduced to explain the charge transport occurring through

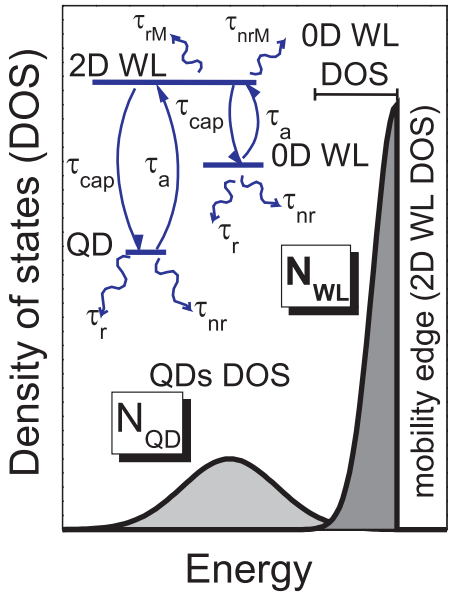

FIG. 3. (Color online) Schematic representation of the carrier dynamics model in the self-assembled QD system with large density of 0D WL states.

the carrier jumps between 0D confined states in a spatially disordered system.[44] Within the presented model, the *e-h* pair dynamics is governed mainly by temperature-driven capture and release processes within distributions of 0D WL and QD states in the vicinity of the 2D WL channel. To keep the model rationality, we do not include direct spatial correlation between the 0D confined states, which enlarge the amount of model parameters considerably. This issue is represented by varying the number of 0D WL states for a constant number of QDs.

Our model is constructed under an important assumption that a direct lateral carrier transfer between 0D states is strongly suppressed. This is justified in the regime of relatively low QD and 0D WL surface densities, low temperature and low photoinjected carrier population, which is in very good agreement with the experimental conditions. Indeed, for the structure under study, the QD density is $\sim 5 \times 10^9$ cm^{-2}, thus the average distance between two adjacent dots exceeds 100 nm, too far to provide efficient quantum mechanical coupling through the most common interaction mechanisms, e.g., the long-range dipole-dipole[45,46] or charge/exciton tunneling.[47,48]

The mean nearest-neighbor distance between a QD and a 0D WL site as well as between two adjacent 0D WL sites in such a spatially inhomogeneous system is hard, if not impossible, to determine experimentally. Nevertheless, we believe that a direct carrier transfer cannot explain the experimental observations. On the one hand, the QD and 0D WL states are energetically decoupled, as is presented in Fig. 1. The only possible carrier transfer mechanism between them is either resonant via the QD excited states or nonresonant through the phonon-assisted inelastic tunneling and/or multipole interactions.[49] On the other hand, the shallow confining potential of QDs implies the presence of a single confined state, therefore only phonon-mediated carrier transfer mechanisms could play a role under the low density of photoinjected carriers. If so, the PL rise time τ_R^{QD} as a function of temperature should be determined mostly by the Bose distribution function, $n_B = [\exp(E/k_BT) - 1]^{-1}$, according to $1/\tau_R^{QD} \propto W_0(n_B + 1)$, where E is the phonon energy, k_B is the Boltzmann constant, and W_0 is the transition rate at $T \approx 0$ K. Consequently, the transfer mechanism should lead to the reduction of τ_R^{QD} with increasing temperature. This fact, confronted with the experimental evidence presented in Fig. 2(b), suggests that 0D WL to QD direct carrier tunneling can play only a minor role in the observed PL dynamics, at least in the temperature range up to 40–45 K.

The direct lateral carrier transfer between 0D WL sites is a more problematic issue and cannot be fully excluded or experimentally identified. We believe, however, that such a carrier transfer within the 0D WL state distribution will not affect significantly the QD PL kinetics, as will be discussed in more detail below, but it influences a carrier redistribution process in the WL.

Finally, we assume that the modeled carrier dynamics is related to the relaxation of Coulomb bound *e-h* pairs rather than individual carriers. Since the estimated *e-h* binding energy to form an exciton in (In,Ga)As/GaAs QDs is on the level of 15–25 meV (Ref. 50) and the experiment is performed in the temperature range of 10–60 K (k_BT is less than 5.2 meV), the assumption is well supported.

B. Model description

Mathematical representation of the model can be summarized in the following set of rate equations:

$$\frac{dn_M}{dt} = -\frac{n_M}{\tau_{rM}} - \frac{n_M}{\tau_{nrM}} \exp\left(\frac{-E_M^{\mathrm{anr}}}{k_B T}\right) - \frac{n_M}{\tau_{\mathrm{cap}_i}} \sum_i \left(1 - \frac{n_i}{N_i}\right)\rho_i + \sum_i \frac{n_i}{\tau_{a_i}} \exp\left(\frac{-E_i}{k_B T}\right), \tag{1.1}$$

$$\frac{dn_i}{dt} = -\frac{n_i}{\tau_{r_i}} - \frac{n_i}{\tau_{nr_i}} \exp\left(\frac{-E_i^{\mathrm{anr}}}{k_B T}\right) - \frac{n_M}{\tau_{\mathrm{cap}_i}} \rho_i \left(1 - \frac{n_i}{N_i}\right) + \frac{n_i}{\tau_{a_i}} \exp\left(\frac{-E_i}{k_B T}\right). \tag{1.2}$$

Initial model conditions assume that all *e-h* pairs which are injected into the system populate immediately the 2D WL states, namely the mobility edge. The *e-h* density in this state is denoted as n_M and its subsequent time evolution is described by Eq. (1.1). Following this expression, the n_M can be depopulated radiatively with a decay time constant of τ_{r_M}, or nonradiatively, taking into account at least two possible relaxation channels. The first channel provides carrier losses characterized by a time constant of τ_{nr_M}, additionally modulated by the temperature-dependent factor of $\exp(\frac{-E_M^{\mathrm{anr}}}{k_B T})$. Here, the E_M^{anr} accounts for the energy threshold above which *e-h* pairs are irreversibly lost due to their interaction with, i.e., crystal lattice or defect states. The second nonradiative recombination channel is described by the third term of Eq. (1.1). It accounts for the carrier capture probability by some distribution of QD or WL localized states. In this term, τ_{cap_i} is the capture time to N_i states constrained to the energy interval of $\Delta E_i = (E_i, E_i + \delta E)$ ($\delta E = 1$ meV), so N_i stands for the "local" density of states. Additionally, the capture probability is governed by the occupation factor $(1 - \frac{n_i}{N_i})$ within the "local" DOS and finally by the ratio of the "local" and total 0D DOS: $\rho_i = \frac{N_i}{N_{\mathrm{QD}} + N_{\mathrm{WL}}}$. The total 0D DOS consists of the 0D QD DOS, N_{QD}, and the 0D WL DOS, N_{WL}. The N_{QD} and N_{WL} can be set independently. Their distribution function is assumed to be Gaussian with a full width at half-maximum equal to 30 and 7 meV, respectively. Additionally, the distribution of the 0D WL states has been cut off at the energy corresponding to the mobility edge, as is shown in Fig. 3. The maximum of the QD distribution is shifted by 50 meV with respect to the mobility edge. All those characteristic energies assumed in the model are supported by the PL experiment.

Although the above-described electron-hole pair relaxation channels provide carrier losses to mobility edge population, these processes are partially reversible. Carriers previously trapped by localized states can be retrieved partially thanks to their coupling to the rising phonon bath caused by the temperature increase. This mechanism is enclosed in the last term of Eq. (1.1). Carrier release from localized states is defined as a function of the release time, τ_{a_i}, modulated by the Boltzmann factor, where E_i stands for the depth of the carrier confinement potential.

The temperature-controlled evolution for each of the "local" *e-h* pair populations n_i limited to the energy interval ΔE_i, as defined earlier, is in turn described by Eq. (1.2). Similarly to Eq. (1.1), the first term is responsible for the spontaneous emission process occurring with the characteristic decay time constant of τ_{r_i}. The second term describes temperature-mediated nonradiative losses to the n_i, where E_i^{anr} is the threshold energy. Finally, the third and fourth terms describe the temperature-dependent carrier capture and release from 0D states, namely the hopping transport between these states. The set of rate equations (1) has been solved numerically for parameters based on experimental and theoretical data presented in Table I.

TABLE I. Set of parameters used in the simulations.

	τ_{r_i} (ps)	τ_{nr_i} (ps)	τ_{cap} (ps)	τ_a (ps)	E^{anr} (meV)
2D WL	200	50	20	20	6
0D WL	400	50	20	20	6
QD	350	50	20	20	15

Since the 2D WL electron-hole pair recombination time cannot be directly taken from the TRPL experiment, it is assumed to be of the order of 200 ps, according to calculations presented in Ref. 51. Also, the 0D WL recombination time has been slightly tuned from 280 ps as measured to 400 ps. This modification is justified due to the fact that even at low temperature there can exist a coupling between the 0D WL sites which can lead to the shortening of measured PL decay time. However, as we have checked, the τ_{r_i} for the 0D WL states can be tuned between 200 and 500 ps without altering the simulation results significantly.

V. DISCUSSION

Figure 4 presents the simulated temperature evolution of the *e-h* pair population rise and decay time at one of the energy positions corresponding to the QD [Figs. 4(a) and 4(c)] and the 0D WL DOS [Figs. 4(b) and 4(d)]. The results are displayed as obtained for three different conditions: (i) the number of 0D WL states exceeds slightly the number of QDs

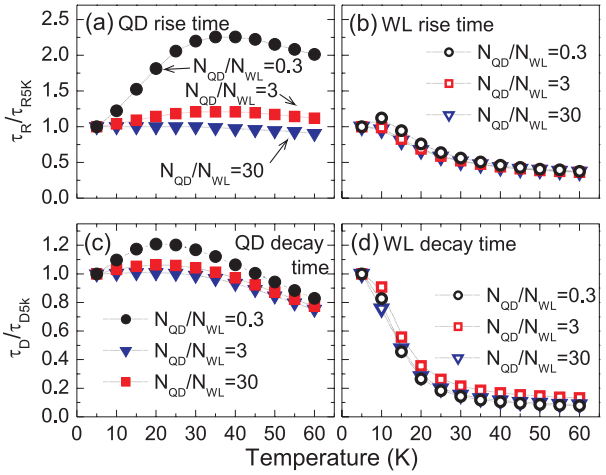

FIG. 4. (Color online) (a) and (b) Theoretically predicted temperature evolution of *e-h* population buildup time for QD (a) and WL (b). (c) and (d) The *e-h* population decay time for QD (c) and WL (d). Data are plotted as a function of three different $N_{\mathrm{QD}}/N_{\mathrm{WL}}$ ratios: 0.3, 3, and 30. Points are collected for the number of QD and WL states fixed, respectively, at 50 and 3 meV below the 2D WL mobility edge.

($N_{QD}/N_{WL} = 0.3$); (ii) the number of 0D WL states is slightly smaller than the number of QDs ($N_{QD}/N_{WL} = 3$); and (iii) the number of QDs exceeds greatly the number of 0D WL states ($N_{QD}/N_{WL} = 30$). Qualitative comparison of the experimental results presented in Figs. 2(b) and 2(d) with the theoretical one in Fig. 4 leads to the conclusion that both characteristics follow very similar trends, as far as $N_{WL} > N_{QD}$. This is particularly important in the context of QD PL kinetics and the atypical temperature behavior of the PL rise time. These results suggest that the number of 0D states in the WL and their intrinsic carrier dynamics can affect strongly the temperature-dependent *e-h* population buildup process in QDs.

To understand the physical background responsible for the increase of the QD PL rise time presented in Fig. 2(b), we have to consider a temperature-driven carrier hopping transport between 0D states of different confinement depths and spatial arrangements. In the system under study, the 0D WL DOS spreads only over a few meV below the 2D mobility channel, thus the most probable mechanism for the carrier to be captured and released by the 0D WL or QD sites occurs through single or multi-acoustic-phonon emission and absorption.[52,53] In the following model, the spatial arrangement of the localized 0D sites is partially simulated by varying the number of 0D WL states (a single confined state per site) in the regime of low QD density. If N_{WL} is much less than N_{QD}, it is more likely that a carrier once released from the 0D WL site to the 2D mobility channel will again be captured by the QD rather than by another 0D WL site. As temperature rises, the efficiency of the exciton-phonon interaction increases, and this controls mainly the observed carrier dynamics. Therefore, in a typical self-assembled QD system in which the condition $N_{QD} \gg N_{WL}$ is fulfilled, the decrease of the QD PL rise time with increasing temperature is observed.[54,55] The QD carrier relaxation scenario can change dramatically when the number of 0D WL states exceeds significantly the number of QDs. At low temperature, the carrier-phonon scattering process is less effective. Once a carrier is released from the confinement potential of a 0D WL site, most likely it will be captured by another 0D WL site rather than by a QD due to the difference in the density of 0D WL sites and QDs ($N_{QD} \ll N_{WL}$). It is expected that before a carrier is recaptured by a QD, it will experience several jump acts in random directions. The underlying processes are time-consuming and involve multiple carrier-acoustic-phonon scattering events. To explain quantitatively the elongation of the WL-to-QD GS relaxation time with temperature, we have to consider the temperature-enhanced process of transferring carriers from the WL states to the dots. Since the QD *e-h* pair recombination lifetime (350 ps) is much longer than the WL-to-QD GS relaxation time (up to ~160 ps), this reduces the number of available dot states (empty dots) for further WL-QD transfer. The higher the temperature is (up to a certain limit related mostly to thermal ionization of QDs), the smaller is the number of QDs which can acquire the excitons from the WL, and hence the longer it takes to transfer carriers from the WL states to the dots. Consequently, it should lead to the increase of the QD PL rise time as observed experimentally in Fig. 2(b) and simulated numerically in Fig. 4(a).

It is worth mentioning that the presented model also predicts the experimentally observed QD and WL PL decay kinetics, and partially the WL PL rise time, which additionally confirms the validity of the model and its generality. Figure 4(b) shows the 0D WL *e-h* population rise time versus temperature. In the system with a number of 0D WL states larger than the population of QDs, the drop of the WL rise time with increasing temperature is preceded by a slow change in the low-temperature limit (5–15 K). A similar picture is presented for experimental data in Fig. 2(b) (open circles). This initial slow down of the buildup of the 0D WL state *e-h* population is attributed to the inefficient carrier capture by the QDs governed by multiple jumps of *e-h* pairs within the ensemble of 0D WL states.

The QD PL decay time presented in Fig. 2(d) (closed circles) is also well recovered qualitatively by the numerical data in Fig. 4(c) (closed circles) in the limit of $N_{QD} < N_{WL}$. Initially, in the temperature range up to about 30–40 K, the *e-h* population decay process in QDs is decelerating. This trend is reversed at higher temperatures. Two factors contribute to the initial deceleration of the *e-h* population decay process. The first one is related to the increasing number of QDs of a given confinement energy depth, thus changing the statistics of the QDs participating in the observed kinetics. The second one is related to recovery of the QD *e-h* population by trapping carriers from 2D WL states which were previously thermally activated from shallow 0D WL states or QDs. At elevated temperatures, the QD population decay time becomes driven by irreversible, nonradiative recombination processes.

The last issue to address is the measured WL decay time as presented in Fig. 2(d) (open circles) and simulated in Fig. 4(d). A certain difference can be observed between the measured and simulated decay time constants. While the measured WL decay time drops slowly in the temperature range of 10–60 K, the simulated curves show a much more pronounced decrease of the population buildup time. This difference can be attributed to the lack of lateral carrier transfer between 0D WL states in the current model, which can take place in the real system. Either resonant or nonresonant exciton transfer between 0D WL states can cause a slow down of the WL decay time by constant refilling of empty 0D WL states. Nevertheless, these data confirm that the possible lateral coupling between 0D WL states does not influence strongly the character of the QD PL rise time temperature dependence.

The results of simulation presented in Fig. 4(b) are related to a small set of localized states defined at a specific ΔE_i within the QD distribution. However, the QD population buildup time should have temperature-sensitive dispersion simply due to different localization depths of electron-hole pairs across the QD or WL distributions. The experimentally obtained dispersion of the PL rise times across the emission energy scale is presented in Fig. 5(a). Figures 5(b) and 5(c) present the calculated dispersion of the electron-hole pair population buildup time on the 0D states being a function of temperature for two initial conditions: $N_{QD} < N_{WL}$ [Fig. 5(b)] and $N_{QD} > N_{WL}$ [Fig. 5(c)]. If $N_{QD} < N_{WL}$, the dispersion of the population buildup time resembles very well the experimental temperature characteristics, especially in the low-temperature regime up to 30 K. At high temperature, there still exists some discrepancy between the simulated and experimental results: the TRPL traces measured at $T > 40$ K show an increase in the PL rise time toward the low-energy side, while the model predicts nearly constant carrier population

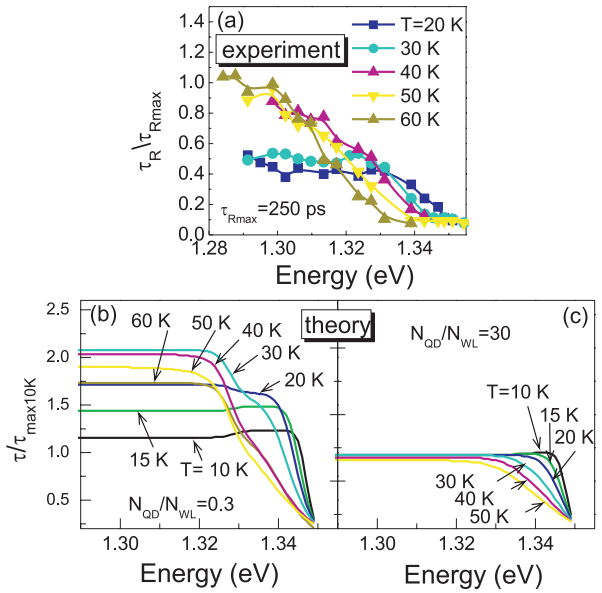

FIG. 5. (Color online) (a) Dispersion of the PL rise time vs temperature across the emission energy. (b) and (c) Numerical calculation of the dispersion of the *e-h* population buildup time for two initial model conditions of $N_{\mathrm{QD}}/N_{\mathrm{WL}} = 0.3$ (b) and $N_{\mathrm{QD}}/N_{\mathrm{WL}} = 30$ (c).

buildup time. Such apparent differences come from the QD population statistics assumed in the model. Most likely the real QD distribution in the given structure deviates from the Gaussian-like distribution. The number of smaller QDs with high energy of the ground-state transition exceeds the number of larger dots which emit photons of lower energy. At elevated temperatures ($T > 40$ K) the carrier dynamics is mostly determined by the carrier exchange between QDs and the 2D mobility edge. Therefore, the experimentally observed continuous increase in the PL rise time toward low energy can be governed by carrier hopping acts over the ensemble of high-energy QDs.

VI. CONCLUSION

To conclude, we have performed studies of carrier dynamics in low indium content, large and elongated self-assembled (In,Ga)As/GaAs quantum dots formed on the wetting layer. The PL experiment indicates the carrier localization within the WL and the temperature-driven transfer between WL and QD states. The temperature-dependent TRPL experiment shows an unusual increase in the QD PL rise time with temperature. Our findings can be explained by a temperature-activated electron-hole pair transfer model. It has been implemented in the form of a set of multilevel rate equations. The model assumes carrier redistribution over two separate sets of QD and 0D WL states of significantly different densities, connected by the two-dimensional mobility channel. We have shown that the slow transfer rate between 0D WL states and QDs is related to time-consuming, acoustic-phonon-mediated carrier jumps between the large density of 0D WL states in the vicinity of the 2D mobility channel.

ACKNOWLEDGMENTS

This work has been supported by the Polish Ministry of Science and Higher Education/the National Science Center Grants No. N N202 181238, No. 2011/01/B/ST3/02379, and No. N N515 496640. The work has been performed employing the NLTK project infrastructure POIG. 02.02.00-003/08-00. The authors acknowledge also the financial support from the COPERNICUS Award of the Fundation for Polish Science and Deutsche Forschungsgemeinschaft.

*marcin.syperek@pwr.wroc.pl

†Present address: Institut für Festkörperphysik, Technische Universität Berlin, Hardenbergstrae 36, D-10623 Berlin, Germany.

[1] *Semiconductor Quantum Dots*, edited by Y. Masumoto and T. Takagahara (Springer-Verlag, Berlin, 2002).

[2] *Single Semiconductor Quantum Dots*, edited by P. Michler (Springer-Verlag, Berlin, 2009).

[3] *Nano-Optoelectronics Concepts, Physics and Devices*, edited by M. Grundmann (Springer-Verlag, Berlin, 2002).

[4] *Semiconductor Quantum Bits*, edited by F. Henneberger and O. Benson (World Scientific, Singapore, 2008).

[5] J. P. Reithmaier, G. Sęk, A. Löffler, C. Hofmann, S. Kuhn, S. Reitzenstein, L. Keldysh, V. Kulakovskii, T. L. Reinecke, and A. Forchel, Nature (London) **432**, 197 (2004).

[6] S. Reitzenstein, A. Bazhenov, A. Gorbunov, C. Hofmann, S. Mnch, A. Löffler, M. Kamp, J. P. Reithmaier, V. D. Kulakovskii, and A. Forchel, Appl. Phys. Lett. **89**, 051107 (2006).

[7] S. M. Ulrich, C. Gies, S. Ates, J. Wiersig, S. Reitzenstein, C. Hofmann, A. Löffler, A. Forchel, F. Jahnke, and P. Michler, Phys. Rev. Lett. **98**, 043906 (2007).

[8] D. Press, S. Götzinger, S. Reitzenstein, C. Hofmann, A. Löffler, M. Kamp, A. Forchel, and Y. Yamamoto, Phys. Rev. Lett. **98**, 117402 (2007).

[9] T. Heindel, C. Schneider, M. Lermer, S. H. Kwon, T. Braun, S. Reitzenstein, S. Höfling, M. Kamp, and A. Forchel, Appl. Phys. Lett. **96**, 011107 (2010).

[10] T. S. Shamirzaev, D. S. Abramkin, A. V. Nenashev, K. S. Zhuravlev, F. Trojanek, B. Dzurnak, and P. Maly, Nanotechnology **21**, 155703 (2010).

[11] Y. Toda, O. Moriwaki, M. Nishioka, and Y. Arakawa, Phys. Rev. Lett. **82**, 4114 (1999).

[12] A. Vasanelli, R. Ferreira, and G. Bastard, Phys. Rev. Lett. **89**, 216804 (2002).

[13] B. Urbaszek, E. J. McGhee, M. Krüger, R. J. Warburton, K. Karrai, T. Amand, B. D. Gerardot, P. M. Petroff, and J. M. Garcia, Phys. Rev. B **69**, 035304 (2004).

[14] E. W. Bogaart, J. E. M. Haverkort, T. Mano, T. van Lippen, R. Nötzel, and J. H. Wolter, Phys. Rev. B **72**, 195301 (2005).

[15] S. Fafard, D. Leonard, J. L. Merz, and P. M. Petroff, Appl. Phys. Lett. **65**, 1388 (1994).

[16]H. Lee, W. Yang, and P. C. Sercel, Phys. Rev. B **55**, 9757 (1997).
[17]S. Sanguinetti, M. Henini, M. Grassi Alessi, M. Capizzi, P. Frigeri, and S. Franchi, Phys. Rev. B **60**, 8276 (1999).
[18]C. Lobo, R. Leon, S. Marcinkevicius, W. Yang, P. C. Sercel, X. Z. Liao, J. Zou, and D. J. H. Cockayne, Phys. Rev. B **60**, 16647 (1999).
[19]A. Polimeni, A. Patane, M. Henini, L. Eaves, and P. C. Main, Phys. Rev. B **59**, 5064 (1999).
[20]Y. C. Zhang, C. J. Huang, F. Q. Liu, B. Xu, J. Wu, Y. H. Chen, D. Ding, W. H. Jiang, X. L. Ye, and Z. G. Wang, J. Appl. Phys. **90**, 1973 (2001).
[21]E. C. Le Ru, J. Fack, and R. Murray, Phys. Rev. B **67**, 245318 (2003).
[22]Fei Ding, Y. H. Chen, C. G. Tang, Bo Xu, and Z. G. Wang, Phys. Rev. B **76**, 125404 (2007).
[23]T. Inoshita and H. Sakaki, Phys. Rev. B **46**, 7260 (1992).
[24]P. A. Knipp and T. L. Reinecke, Phys. Rev. B **52**, 5923 (1995).
[25]R. Ferreira and G. Bastard, Appl. Phys. Lett. **74**, 2818 (1999).
[26]U. Bockelmann and T. Egeler, Phys. Rev. B **46**, 15574 (1992).
[27]I. Vurgaftman and J. Singh, Appl. Phys. Lett. **64**, 232 (1994).
[28]A. V. Uskov, J. McInerney, F. Adler, and H. Schweizer, Appl. Phys. Lett. **72**, 58 (1998).
[29]R. Heitz, T. R. Ramachandran, A. Kalburge, Q. Xie, I. Mukhametzhanov, P. Chen, and A. Madhukar, Phys. Rev. Lett. **78**, 4071 (1997).
[30]R. Leon, S. Fafard, P. G. Piva, S. Ruvimov, and Z. Liliental-Weber, Phys. Rev. B **58**, R4262 (1998).
[31]H. D. Robinson, B. B. Goldberg, and J. L. Merz, Phys. Rev. B **64**, 075308 (2001).
[32]E. S. Moskalenko, M. Larsson, W. V. Schoenfeld, P. M. Petroff, and P. O. Holtz, Phys. Rev. B **73**, 155336 (2006).
[33]A. Babinski, J. Borysiuk, S. Kret, M. Czyż, A. Golnik, S. Raymond, and Z. R. Wasilewski, Appl. Phys. Lett. **92**, 171104 (2008).
[34]A. Löffler, J. P. Reithmaier, A. Forchel, A. Sauerwald, D. Peskes, T. Kümmell, and G. Bacher, J. Cryst. Growth **286**, 6 (2006).
[35]P. Poloczek, G. Sęk, J. Misiewicz, A. Löffler, J. P. Reithmaier, and A. Forchel, J. Appl. Phys. **100**, 013503 (2006).
[36]G. Sęk, A. Musiał, P. Podemski, M. Syperek, J. Misiewicz, A. Löffler, S. Höfling, L. Worschech, and A. Forchel, J. Appl. Phys. **107**, 096106 (2010).
[37]S. Reitzenstein, S. Münch, P. Franeck, A. Rahimi-Iman, A. Löffler, S. Höfling, L. Worschech, and A. Forchel, Phys. Rev. Lett. **103**, 127401 (2009).
[38]We assume here that the investigated QDs exhibit rather shallow confining potential with a single quantized state.
[39]T. F. Boggess, L. Zhang, D. G. Deppe, D. L. Huffaker, and C. Cao, Appl. Phys. Lett. **78**, 276 (2001).
[40]L. Zhang, T. F. Boggess, D. G. Deppe, D. L. Huffaker, O. B. Shchekin, and C. Cao, Appl. Phys. Lett. **76**, 1222 (2000).
[41]A. F. G. Monte, F. V. de Sales, J. J. Finley, A. M. Fox, S. W. da Silva, P. C. Morais, M. S. Skolnick, and M. Hopkins, Microelectron. J. **34**, 747 (2003).
[42]K. Güdoŭdu, K. C. Hall, T. F. Boggess, D. G. Deppe, and O. B. Shchekin, Appl. Phys. Lett. **85**, 4570 (2004).
[43]D. Sreenivasan, J. E. M. Haverkort, O. Ipek, B. Martinez-Vazqueze, T. J. Eijkemans, T. Mano, and R. Nötzel, Physica E **40**, 1879 (2008).
[44]N. F. Mott, J. Non-Crystalline Solids **1**, 1 (1968).
[45]T. Förster, Ann. Phys. (Paris) **2**, 55 (1948).
[46]C. R. Kagan, C. B. Murray, and M. G. Bawendi, Phys. Rev. B **54**, 8633 (1996).
[47]P. J. Wiesner, R. A. Street, and H. D. Wolf, Phys. Rev. Lett. **35**, 1366 (1975).
[48]M. Bayer, P. Hawrylak, K. Hinzer, S. Fafard, M. Korkusinski, Z. R. Wasilewski, O. Stern, and A. Forchel, Science **291**, 451 (2001).
[49]T. Miyakawa and D. L. Dexter, Phys. Rev. B **1**, 2961 (1970).
[50]G. A. Narvaez, G. Bester, and A. Zunger, Phys. Rev. B **72**, 245318 (2005).
[51]C. Piermarocchi, F. Tassone, V. Savona, A. Quattropani, and P. Schwendimann, Phys. Rev. B **53**, 15834 (1996).
[52]D. Emin, Phys. Rev. Lett. **32**, 303 (1974).
[53]E. Gorham-Bergeron and David Emin, Phys. Rev. B **15**, 3667 (1977).
[54]B. Ohnesorge, M. Albrecht, J. Oshinowo, A. Forchel, and Y. Arakawa, Phys. Rev. B **54**, 11532 (1996).
[55]A. V. Maleev, I. V. Ignatiev, I. Ya. Gerlovin, I. E. Kozin, and Y. Masumoto, Phys. Rev. B **71**, 195323 (2005).